Supporting Information

Supramolecular Construction of Vesicles Based on Core-Substituted Naphthalene Diimides Bearing TEG Motifs

Sheshanath V. Bhosale,*[a] Chintan H. Jani,[a] Cecilia H. Lalander,[a] Steven J. Langford,[a] Igor Nerush,[b] Joe Shapter,[b] Diego Villamaina,[c] and Eric Vauthey[c]

[a] School of Chemistry, Monash University, Clayton, Australia 3800.
[b] School of Chemistry, Physics and Earth Sciences Flinders University of South Australia -5042
[c] Physical Chemistry Department, Sciences II University of Geneva, 30, Quai Ernest Ansermet CH-1211 Geneva 4 Switzerland

sheshanath.bhosale@monash.edu

Contents

1. Material and measurements

Material and measurements: Catechol, naphthalene tetracarboxy dianhydride, DMF, chloroform, methanol and dichloromethane were purchased from Aldrich and used without purification, unless otherwise specified. UV-vis absorption spectra were recorded on a Perkin Elmer Lambda 40p spectrometer. ^{1}H NMR, ^{13}C-NMR spectra were recorded on a Bruker spectrometer using chloroform-d as solvent and tetramethylsilane as an internal standard. The solvents for spectroscopic studies were of spectroscopic grade and

used as received. Self-assembled samples were prepared by dissolving amphiphilic NDI **1** in respective solvents. The mixed aggregate system was prepared by dissolving NDI **1** in DMSO or mixture of $CHCl_3$ and methanol injected over on it (v/v 6:4). The sample solution was kept at room temperature for few hours before TEM and AFM measurements.

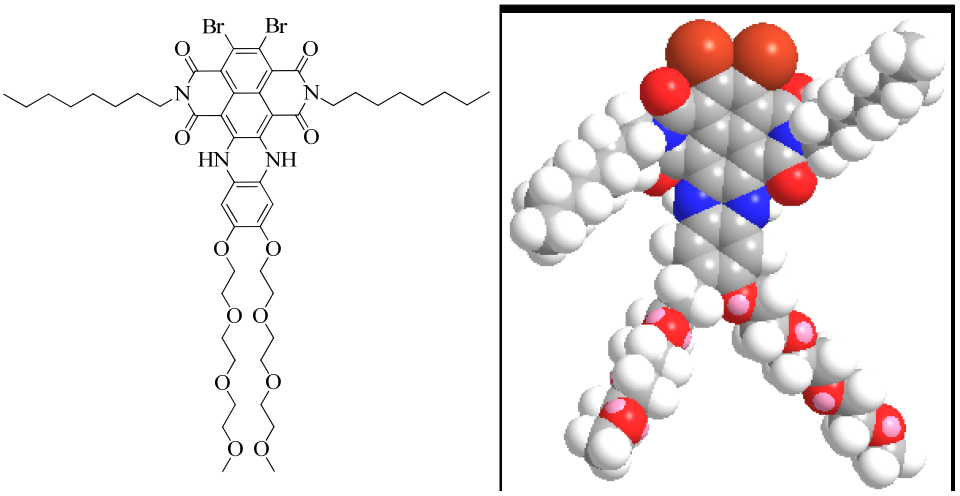

Scheme S1. Molecular structures of **1** and space filling model after *MM2* calculation

2. Synthesis and Characterisation

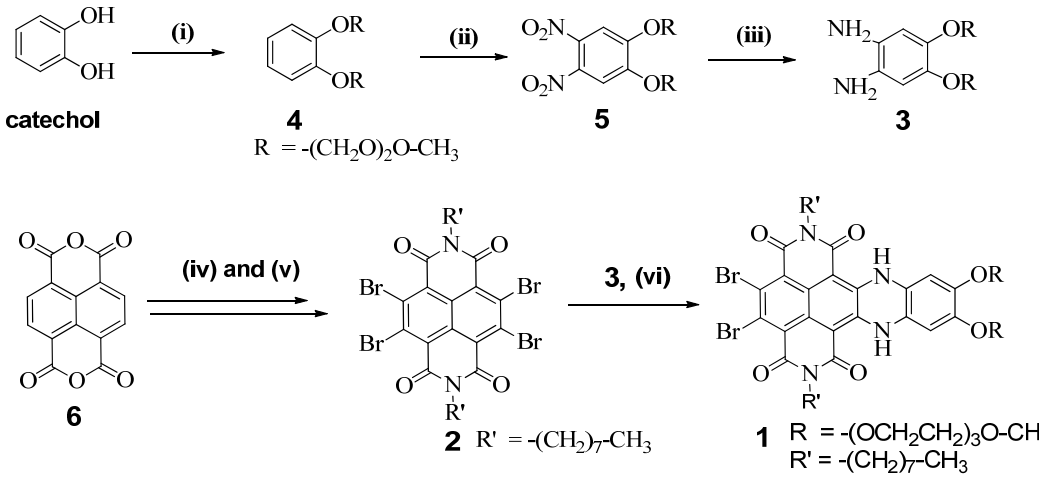

Scheme S2. Synthesis of core-substituted naphthalene diimide **1**. Reagents and conditions: (i) $Cl\text{-}(CH_2CH_2O)_3\text{-}CH_3$, DMF, K_2CO_3, 90 ^oC, 3d; (ii) HNO_3, H_2SO_4, DCM,

16h; (iii) Pd/C, hydrazine hydrate, ethanol, rt. 16h; (iv) 30% SO_3^-, H_2SO_4, NaBr, overnight, 130 ^oC; (v) 1-octylamine, AcOH, 90 ^oC, overnight; (vi) DMF, 135 ^oC, 15 min.

1,2-Bis(2-(2-(2-methoxyethoxy)ethoxy)ethoxy)benzene (4).

Catechol (2.5 g, 0.02 mol) and K_2CO_3 (5.5 g, 0.1 mol) were placed in a two-necked RBF under a nitrogen atmosphere. DMF (100 ml) was added via a syringe. After stirring for 20 min. at room temperature, 1-chloro-2-(2-(2-methoxyethoxy)ethoxy)ethane (12 g, 0.06 mmol) was added and the mixture was heated at 90°C for 2 days. The mixture was allowed to cool down to ambient temperature before pouring into deionised water (100 ml) into it. Diethyl ether (3x60 ml) was used to extract the product and the combined organic phases were dried over $MgSO_4$ and removed *in vacuo*. A yellow oil was obtained which was dried *in vacuo* to obtained **4** (7.0 g, 74%). ^{1}H NMR ($CDCl_3$, 300 MHz) δ 6.88 (m, 4H, ArH), 4.16 (t, J = 6.6 Hz, 4H, O-CH_2), 3.85 (t, J = 6.9 Hz, 4H), 3.4-3.7 (m, 16H), 3.37 (s, 6H); ^{13}CNMR ($CDCl_3$,125MHz) δ 150.7, 120.9, 120.6, , 72.0, 71.3, 70.9, 70.7, 70.5, 69.4, 59.05; MS-EI *m*/*z* 403.5 $((M + 1H)^+$.

1,2-Bis(2-(2-(2-methoxyethoxy)ethoxy)ethoxy)-4,5-dinitrobenzene (5).

To a cooled (15 ^oC) mixture of 4.5 g (0.01 mol) of **4** and 70 mL of glacial acetic acid in 70 mL of dichloromethane was slowly added 10 mL of concentrated nitric acid (65%), while keeping the temperature below 40^oC. After being stirred for 30 min, the solution was again cooled to 15 ^oC, 25 mL of fuming nitric acid (100%) was slowly added, and the mixture was stirred at room temperature for 3 days. The solution was poured into 250 g of ice water, and the organic layer was washed with water (3 × 150 mL), saturated $NaHCO_3$ solution (150 mL), and brine (150 mL). After workup, the mixture was dried

with $MgSO_4$, the solvent was evaporated and dried over vacuum to obtain **5** (4.0 g, 72%) as a semi-liquid. ^{1}H NMR ($CDCl_3$, 300 MHz): δ 7.47 (s, 2H), 4.62 (t, *J* = 6.8 Hz, 4H), 4.33 (t, *J* = 6.4 Hz, 4H), 3.52-3.90 (m, 16H), 3.36 (s, 6H); ^{13}C NMR ($CDCl_3$, 125 MHz) δ 154.2, 134.4, 115.6, 71.6, 70.4, 70.1, 70.0, 69.3, 59.1; MS-EI *m*/*z* 493.4 $(M + H)^+$.

4,5-bis(2-(2-(2-methoxyethoxy)ethoxy)ethoxy)benzene-1,2-diamine (3).

To a solution of of **5** (1.8 g, 3.4 mmol) in 50 mL of ethanol, 0.09 g of 10% Pd/C, and 7.2 mL (36 mmol) of hydrazine monohydrate were added. After overnight of refluxing, the hot solution was filtered over celite, while kept under N_2. After cooling, the white precipitate was filtered off and rinsed with cold, methanol to yield **3** (1.24 g, 78%) as a yellow liquid. ^{1}H NMR ($CDCl_3$, 300 MHz): δ 5.89 (s, 2H), 4.7 (s, br, 4H), 4.32 (t, *J* = 6.7 Hz, 4H), 4.12 (t, *J* = 7.1Hz, 4H); 3.3-3.8 (m, 16H), 3.32 (s, 6H); ^{13}C NMR ($CDCl_3$, 125 MHz) δ 133.8, 128.6, 7, 100.1, 72.0, 71.5, 70.7, 69.6, 59.2; MS-EI *m*/*z* 433.4 $(M+H)^+$.

2,3,6,7-Tetrabromo-dioctyl-naphthalene diimide (2):[1] 2,3,6,7-Tetrabromo-naphthalene

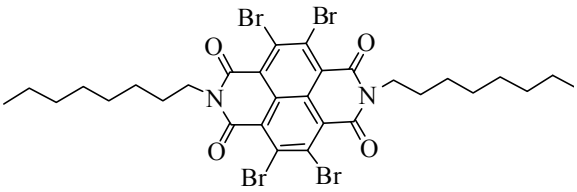

dianhydride was prepared from naphthalene dianhydride by literature method obtained yellow solid with 93% yield.[1] Following literature method compound **2** was synthesized in 30% yield as yellow crystalline solid. M.P. 259 °C. ^{1}H NMR ($CDCl_3$, 300 MHz) δ 4.18-4.23 (t, *J* = 7.7 Hz, 4H), 1.71-1.79 (m, 4H), 1.38-1.41 (m, 8H), 1.28-1.35 (m, 12H), 0.87-0.91 (t, *J* = 6.97, 6H). ^{13}C NMR ($CDCl_3$, 125 MHz) δ 159.7, 135.4, 126.5, 125.7, 42.8, 31.8, 29.21, 29.20, 27.9, 27.1, 22.6, 14.1. FT-IR (KBr, cm^{-1}) *v* 2958, 2921, 2853, 1713, 1666, 1502, 1431,

1409, 1374, 1289, 1178, 1154, 1013, 909, 789, 768, 721, 582, 543. HRMS (ESI) *m/z*: calcd for $C_{30}H_{34}Br_4N_2O_4$ 806.2180, found 806.2176, UV/vis (CH_2Cl_2): λ_{max}/nm (ε/M^{-1} Cm^{-1}) = 427 (10 900), 403 (12 100). Fluorescence (CH_2Cl_2): No fluorescence output. All spectroscopic data matches with literature.[1]

Core-substituted naphthalene diimide (NDI) 1.

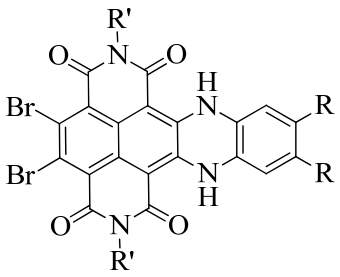

1 R = -$(OCH_2CH_2)_3$-OCH_3
R' = -$(CH_2)_7$-CH_3

A mixture of **2** (100 mg, .12 mmol) and 4,5-bis(2-(2-(2-methoxyethoxy) ethoxy)ethoxy)benzene-1,2-diamine **3** (0.214 mg, 0.49 mmol) in dry DMF (2 mL) were heated at 135°C for 15 min. (colour change was observed yellowish to dark green), and completion of the reaction was monitored by TLC. After completion DMF was removed on a rotary evaporator, and the residue purified by column chromatography on flash silica using 9:0.5 DCM/MeOH. Dark green crystals were obtained **1** (102 mg, 76%). ^{1}H NMR ($CDCl_3$, 400 MHz) δ 13.39 (s, 2H), 6.91 (s, 2H), 4.17 (m, 4H), 4.05 (t, *J* = 7.8, 4H), 3.93 (t, *J* = 6.8, 4H), 3.39-3.92 (m, 16H), 3.25 (s, 6H), 1.88 (m, 4H), 1.31 (m, 20H), 0.87 (m, 6H); ^{13}C NMR ($CDCl_3$, 125 MHz) δ 164.5, 164.1, 161.5, 160.0, 156.5, 155.1, 148.3, 142.1, 131.2, 129.2, 127.7, 126.0, 121.2, 121.1, 120.5, 94.1, 72.0, 70.9, 70.7, 70.6, 69.5, 59.0, 41.2, 31.8, 29.7, 29.4, 29.3, 29.2, 27.8, 27.3, 22.6, 14.1; HRMS (ESI) *m/z*: calcd for

$C_{50}H_{68}Br_2N_4O_{12}$ 1076.9025, found 1076.9025; FT-IR (KBr, Cm^{-1}) *v* 2959, 2925, 2852, 1716, 1666, 1502, 1431, 1409, 1374, 1287, 1173, 1157, 1013, 910, 789, 768, 721, 582, 545; UV/vis (CH_2Cl_2): λ_{max}/nm ($\varepsilon/M^{-1}Cm^{-1}$) = 644 (36 000), 582 (15 550), 538 (5400), 431 (25 750), 408 (12 700), 388 (4250); Fluorescence (CH_2Cl_2): λ_{max} 699, 647 (λ_{ex} = 571 nm).

3. UV-vis absorption spectroscopy

Stock solutions (concentration $1x10^{-3}$ M) of NDI **1** dye were made in $CHCl_3$. A 0.2 mL aliquot of the stock solution was transferred to two different volumetric flasks of $CHCl_3$ and DMSO, each of 2 mL volume. The solutions were allowed to equilibrate for 2 h prior to the spectroscopic measurements. For variable-temperature UV-visible spectroscopic experiments, a 25 min interval was given before each measurement after the desired temperature was reached.

Figure S1 shows the absorption spectra of NDI **1** with temperature dependent changes in DMSO. The latter is a good solvent for solvation of the π system of NDI dyes, hence the dyes do not form aggregates at a high $CHCl_3$ 90% content at the concentration ($1x10^{-4}$ M) applied in these experiments. Thus, for a $CHCl_3$/MeOH (*v/v,* 9:1) ratio the major absorption band shows the well-resolved vibronic structure ranging from 410 to 660 nm that is characteristic for the S0→S1 transition of the isolated NDIs chromophore. In contrast, methanol is a bad solvent for the solvation of the π system of NDI. As a consequence, the dye is not soluble in pure MeOH and aggregation is observed at higher volume ratios of $CHCl_3$/MeOH as evidenced by distinct spectral changes. The most prominent features are a reduction in the peak intensity along with a significant blueshift of the absorption maximum and a loss of the fine structure. These features suggest the

formation of face-to-face π stacks of rotationally displaced NDI chromophores, similar effect observed in the case of perylenediimides[2] and other systems[3].

Heating the suspension up to 70 °C caused a gradual change in absorption spectra, with increasing absorption band. Above 70 °C, most of the NDI molecules are freely dispersed in the solvent (see Figure S1).

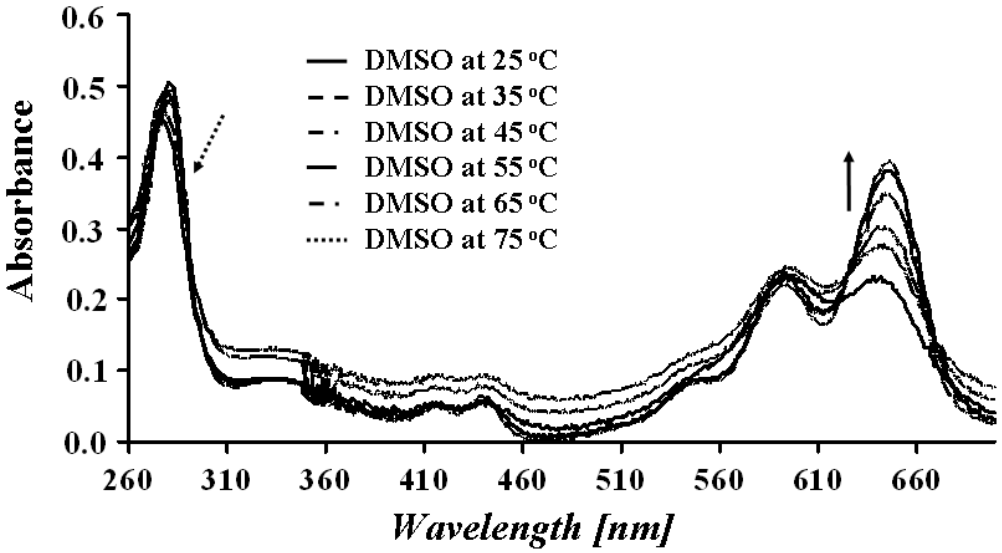

Figure S1.UV/vis spectroscopy of NDI **1** in DMSO at different temperatures, arrow indicates changes upon increasing temperature.

4. Transmission electron microscopy (TEM) of NDIs 1

TEM measurements were performed on an electron microscopy Igor 1200EX, operating at an accelerating voltage of 80 kV. 0.5 Microlitre of freshly prepared sample solution ($1x10^{-4}$ M in DMSO) was dropped onto a TEM grid (400-mesh copper grid coated with carbon) and the solvent was allowed to evaporate before introduction into the vacuum system. Negative stained was performed by addition of a drop of uranyl acetate onto the carbon grid, after few min. remaining solvent was removed by tapping with filter paper and images were collected.

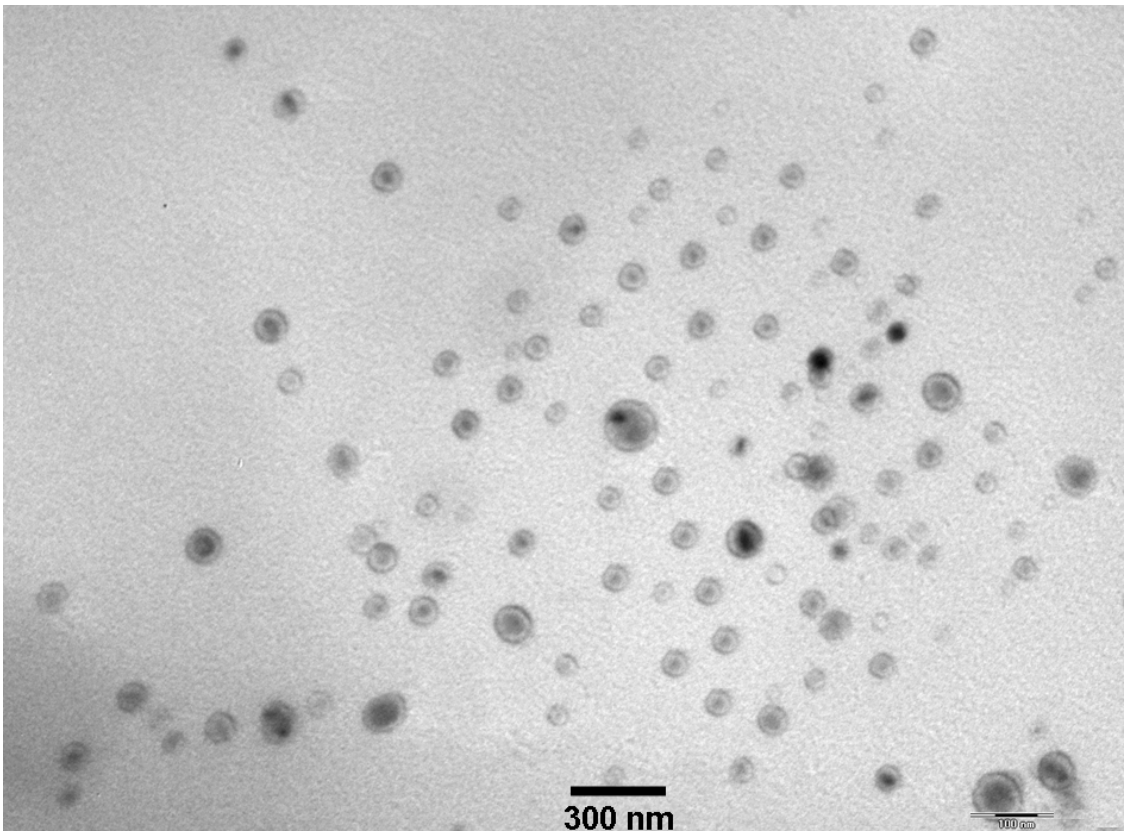

Figure S2a. TEM image of NDI **1** prepared from DMSO solution and stained with uranyl acetate. The scale bar represents 300 nm.

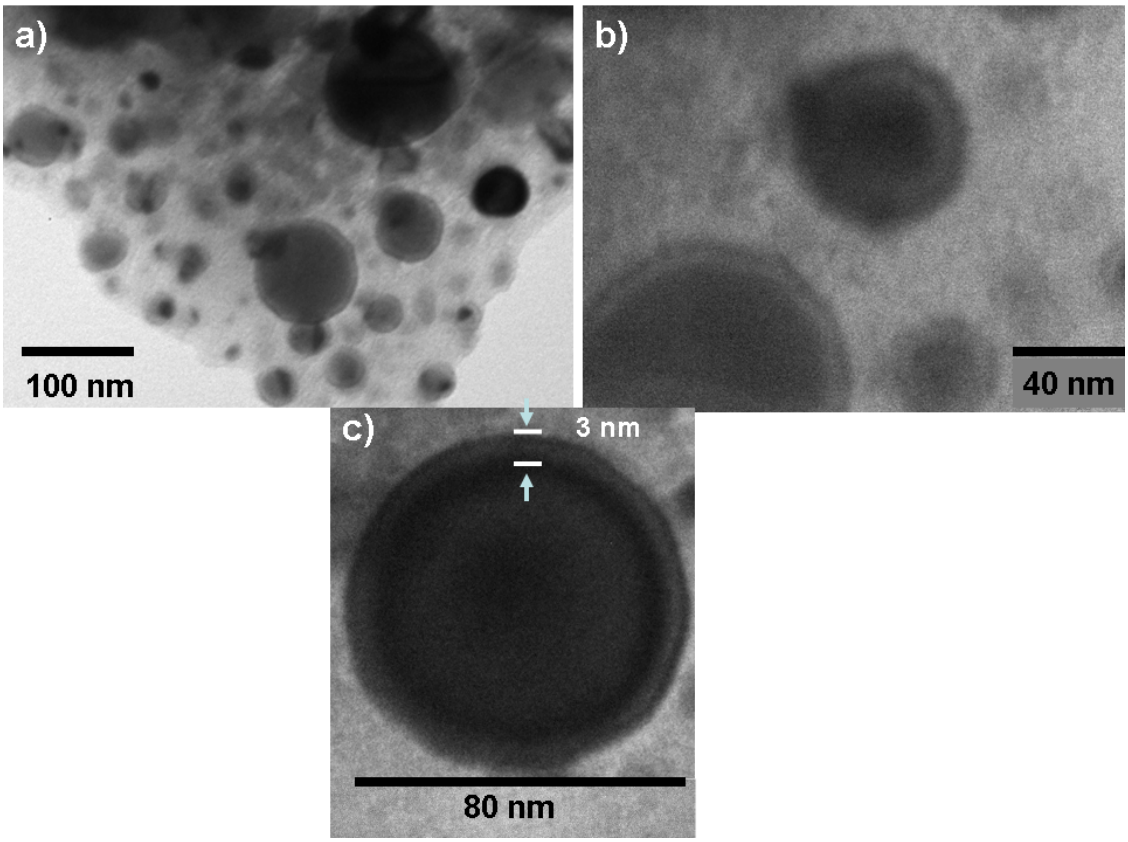

Figure S2b. High magnification TEM image of c-NDI **1** prepared from DMSO solution and stained with uranyl acetate a) and b), the scale bar represents 100 and 40 nm respectively. Single vesicles to identify the interlamellar spacing between two adjacent layers c, the scale bar represents 80 nm.

5. Atomic force microscopy (AFM) of NDIs 1

The samples were characterised using an Atomic Force Microscope (AFM) from Agilent Technologies (5500 AFM). Micromach Ultrasharp probes with silica wafer coating for enhanced reflectivity (NSC15/AIBS), with a typical resonance frequency of 325 kHz and a force constant of 40 N/m, were used for imaging. Sample of NDIs were prepared by spin-coating the freshly prepared solution ($1x10^{-4}$ M in dry DMSO) onto silica coating at 2000 rpm. The vesicle diameter and height was performed by measuring the mean horizontal distance and height of particles (see Figure 3 in manuscript and Figure S2).

Similar experiment were carried out for mixture of $CHCl_3$/MeOH: Sample of NDIs **1** were prepared by spin-coating the freshly prepared solution ($1x10^{-4}$ M in $CHCl_3$/MeOH v/v 6:4) onto silica coating at 2000 rpm. The vesicle diameter and height was performed by measuring the mean horizontal distance of particles (see figure 4 in manuscript).

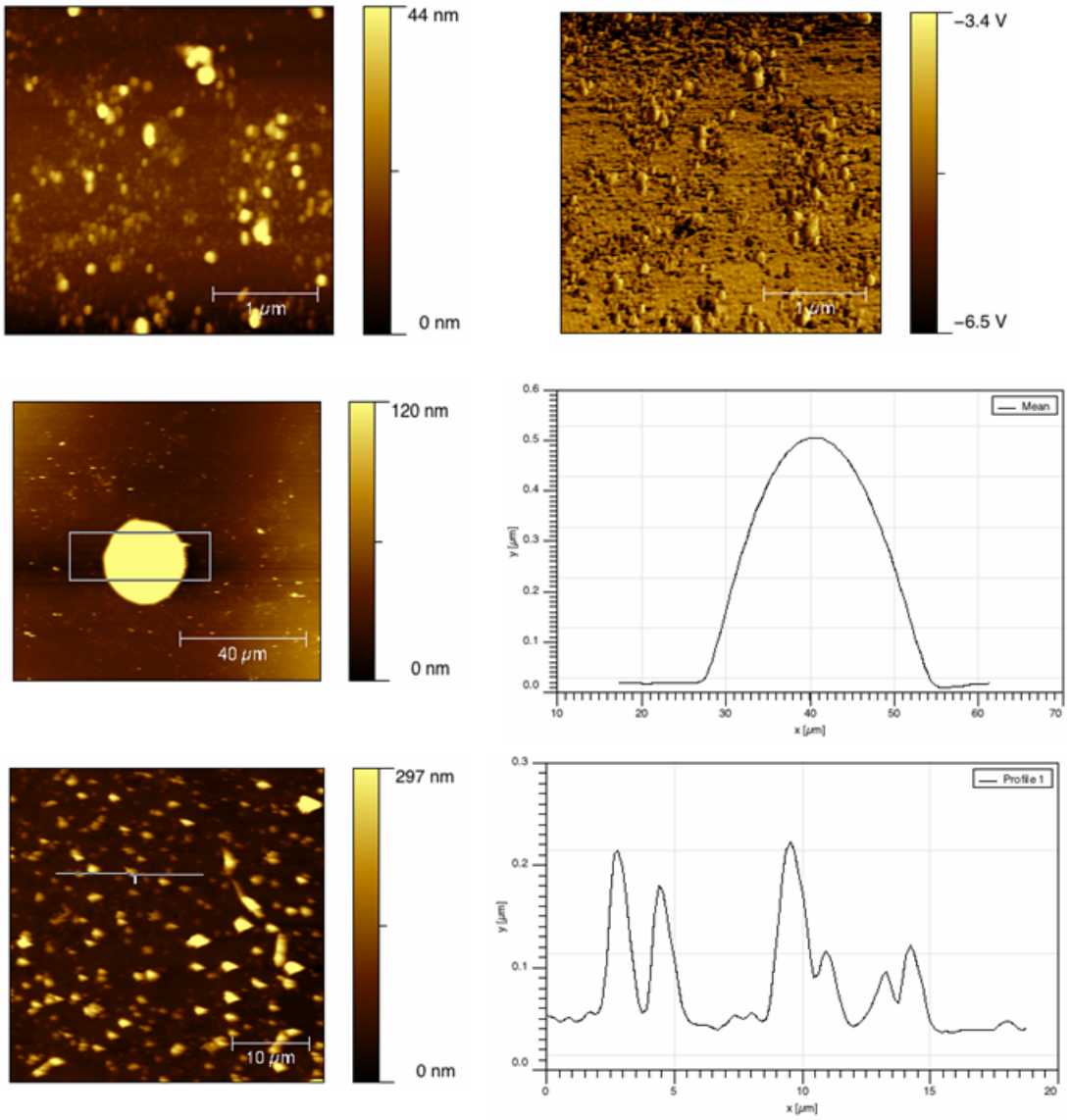

Figure S3: AFM images of vesicles formed by NDIs **1** in DMSO was spin-cast on silica wafer before taking the AFM images: a) height image, b) phase image of a, (c) high magnification height image (e) height images, (d and f) cross-section analysis magnified region from image c and e respectively.

5.1 AFM images of NDI 1 in $CHCl_3$/MeOH

The samples were characterised using an Atomic Force Microscope (AFM) from Agilent Technologies (5500 AFM). Micromach Ultrasharp probes with silica wafer coating for enhanced reflectivity (NSC15/AIBS), with a typical resonance frequency of 325 kHz and a force constant of 40 N/m, were used for imaging. The vesicle diameter and height was performed by measuring the mean horizontal distance and height of particles. It can be found that all the compounds self-assembled into spherical vesicles, the average height was estimated to be c.a. 14 nm (Figure S4), is smaller than that vesicles formed from DMSO, average height of particles is c.a. 25-35 nm (Figure S4). This result may be due to the fact that the removal of $CHCl_3$ and MeOH solvent molecules easy to squeeze from the hollow spheres and also the high local force applied by the AFM tip drags.

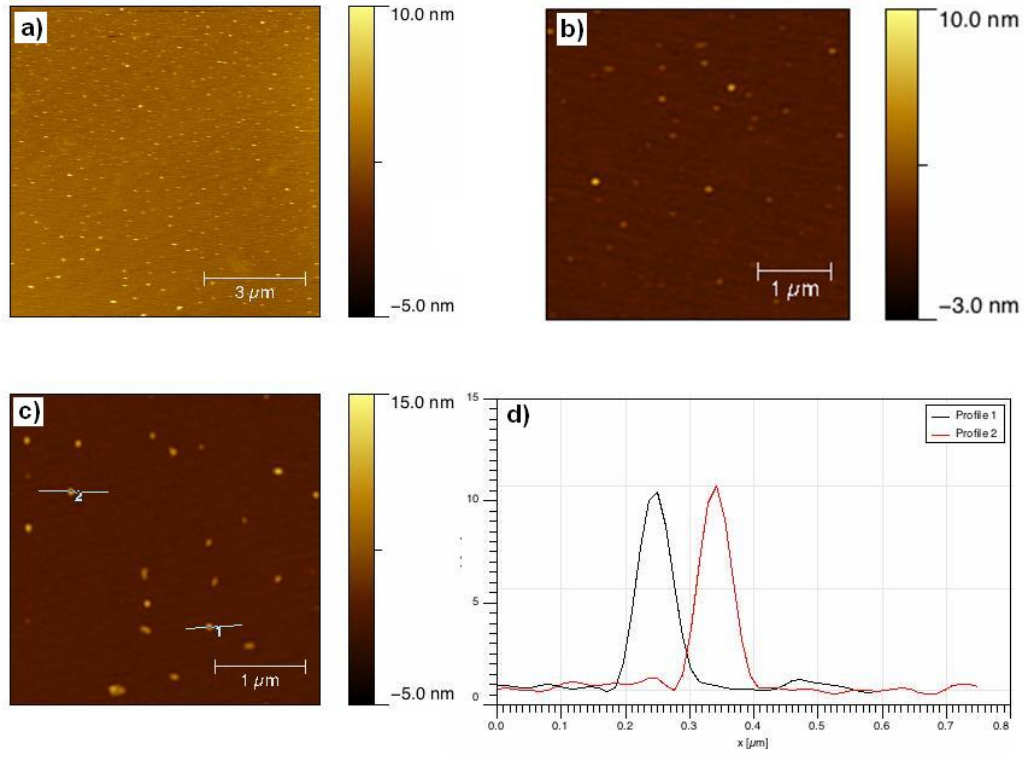

Figure S4: AFM images showing evolution of self-assembling supramolecular structures of **1** ($1x10^{-4}$) in 40% v/v methanol/chloroform (a-c) and (d) shows height profile for c.

6. Dynamic light scattering (DLS)

Dynamic light scattering (DLS) measurements were performed using a Malvern Nano-ZS zetasizer (Malvern Instruments Ltd, Worcestershire, United Kingdom). The Nano-ZS employs non-invasive back scatter (NIBS™) optical technology and measures real time changes in intensity of scattered light as a result of particles undergoing Brownian motion. The sample is illuminated by a 633 nm He–Ne laser and a maximum output power of 4 mW power was used as light source. Measurements were performed at scattered light is measured at a 173° accumulation angle. The size distribution of the vesicles is calculated from the diffusion coefficient of the particles according to Stokes-Einstein equation. The average diameter and the polydispersity index of the samples are calculated by the software using CONTIN analysis.[4] Freshly prepared samples of **NDI 1** with a concentration of $1x10^{-4}$ M in DMSO or $CHCl_3$/MeOH (6:4, v/v) were used for DLS measurements. The sample was equilibrated for 5 min at the set temperature each time. Dynamic Light Scattering measurements show the existence of aggregates with R_h = 90-115 nm in coexistence with several larger and smaller sized species. The radius of the vesicles falls typically in the range ~100 nm, but varies in the range 90–115 nm, depending on the conditions of the preparation. The relative amount of the two species depends on concentration and time but it was not possible to remove the larger particles by filtration or any other common method. In this manuscript we focus on the analysis of the "primary" R_h = 100 nm assemblies. However, due to the presence of the small amounts of the larger aggregates, it is not possible to further characterize the smaller species by static light scattering. Measurements were also performed with a high sample concentration $1x10^{-3}$ M and $1x10^{-2}$ M. The results were the same as with the $1x10^{-4}$ M solution. However vesicles formed in mixed solvent $CHCl_3$/MeOH (6:4, v/v) gives R_h = 17-20 nm assemblies.

7. Steady state absorption spectra

The absorption spectra of NDI **1** recorded in three different solvents ($CHCl_3$, $CHCl_3$/MeOH 6:4 and DMSO) are shown in figure S6.

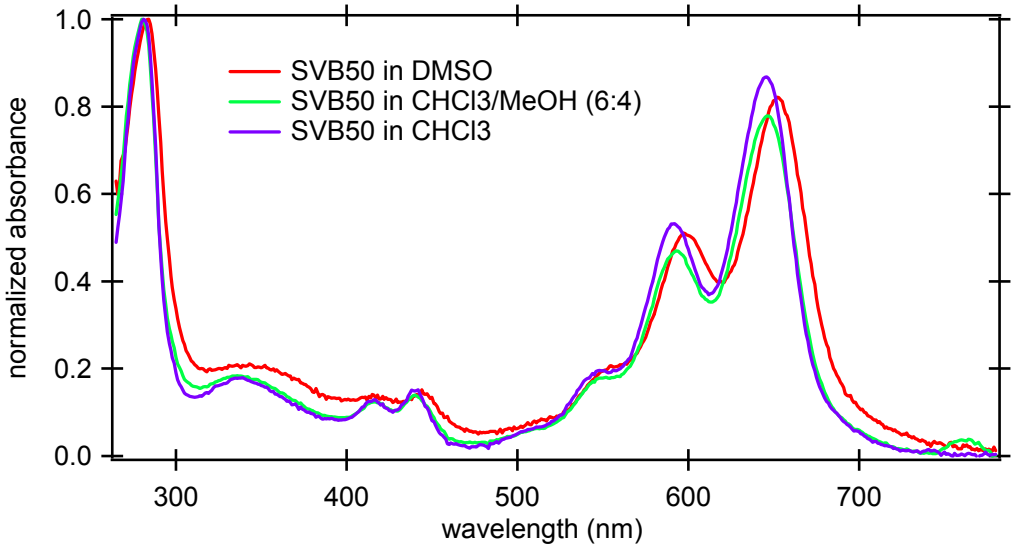

Figure S6. Absorption spectra of NDI **1** recorded directly after sample preparation.

The absorption spectra reported in figure S6 have been recorded directly after the preparation of the samples described above. NDI **1** dissolved in three different solvents shows a structured band in the 500 – 700 nm regions that can be assigned to the $S_1 \leftarrow S_0$ transition. This band is absent in the spectrum of core unsubstitued NDI and can thus be ascribed to a charge transfer type transition involving the core substituents. In both solvents, pure $CHCl_3$ and in the $CHCl_3$/MeOH (6:4) mixture, the absorption maximum is at λ_{abs} = 646 nm. In DMSO, this band exhibits a red shift to λ_{abs} = 652 nm.

The second absorption band (400-450 nm) that can be assigned to the $S_2 \leftarrow S_0$ transition is associated with a π-π* transition involving only the NDI center. The maximum of this band is at λ_{abs}= 440 nm in both $CHCl_3$ and the $CHCl_3$/MeOH mixture, whereas in DMSO it shifts only slightly to λ_{abs}= 442 nm.

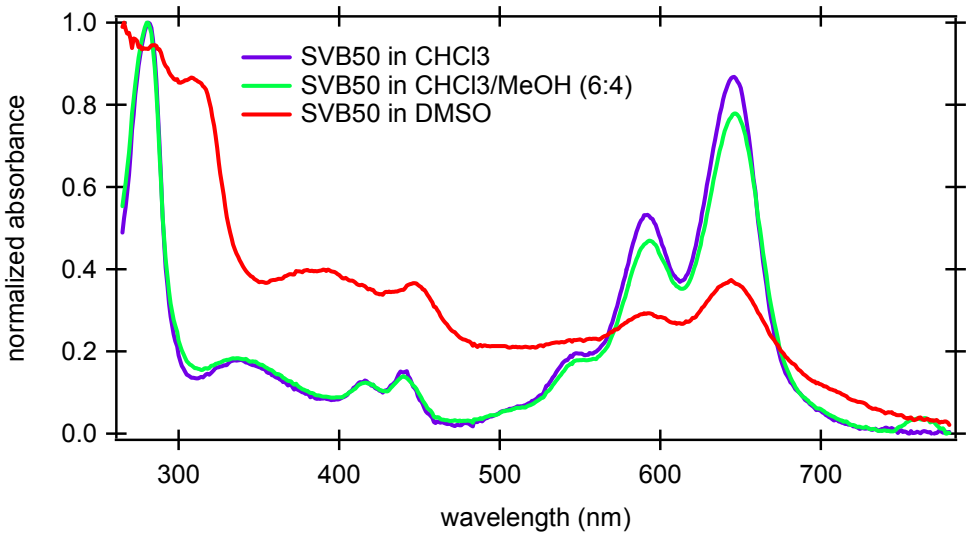

Figure S7. Absorption spectra of NDI **1** recorded 1 day after sample preparation.

The absorption spectra measured 1 day after sample preparation are shown in figure S7. The absorption spectra of **1** recorded in $CHCl_3$ and the $CHCl_3$/MeOH mixture keep the same band shape as in the spectra of the fresh samples. Moreover, the absorption maxima are essentially unchanged. The band shape of absorption spectrum of **1** in DMSO differs from that recorded soon after sample preparation. In particular the $S_1 \leftarrow S_0$ band becomes less structured and broader and its maximum is blue-shifted (λ_{abs}= 644 nm).

After a few days, the solution of NDI **1** in DMSO looses totally its colour. As shown in figure S8, the band becomes less structured and broader with time. Such variation could point to the formation of larger vesicles aggregate.

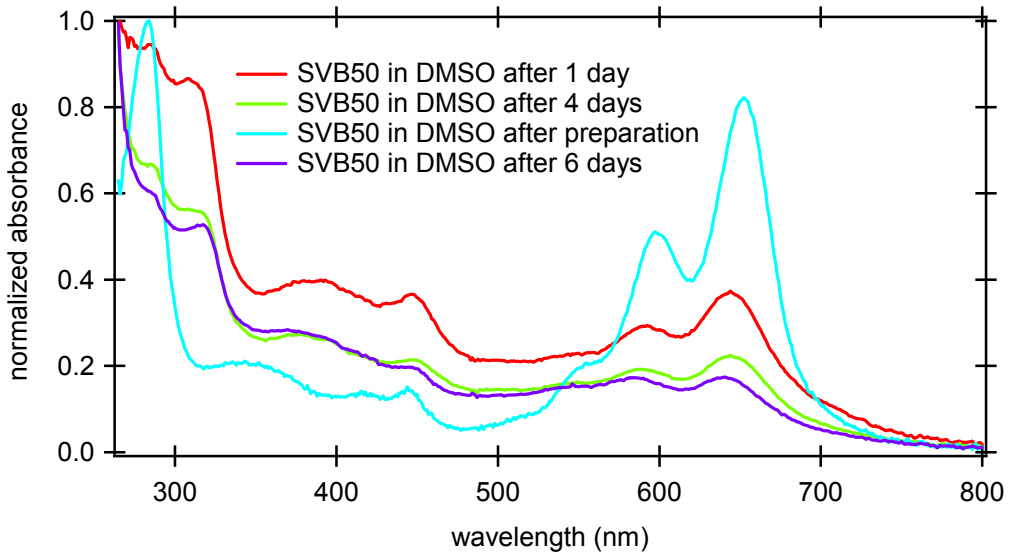

Figure S8. Absorption spectra of NDI **1** in DMSO recorded at different times after sample preparation

8. Stead state fluorescence spectra

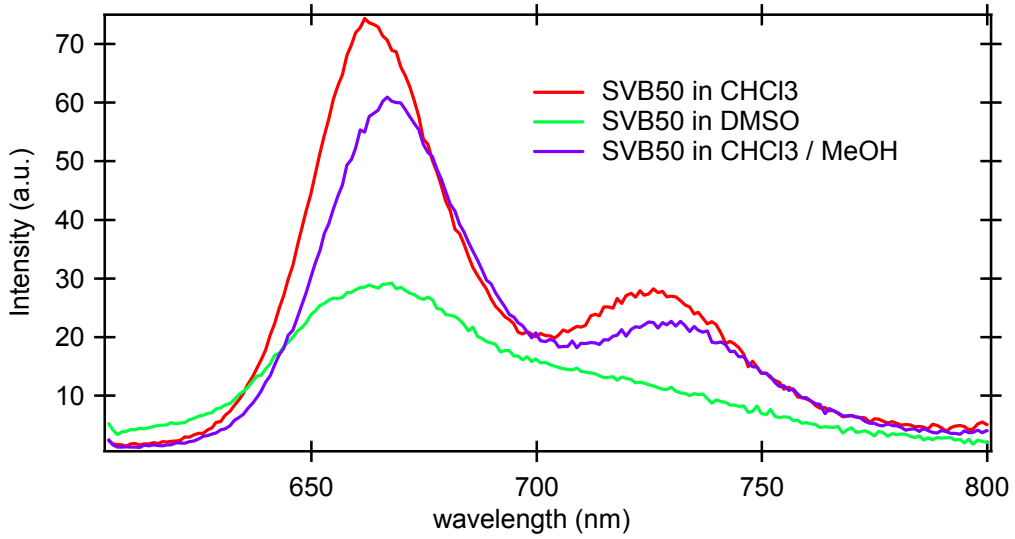

Figure S9. Fluorescence spectra of NDI **1**, λ_{ex} = 600 nm

The fluorescence spectra of **1** recorded 1 day after sample preparation in three solvents upon excitation at 600 nm in the $S_1 \leftarrow S_0$ absorption band are shown in figure S9. In $CHCl_3$, **1** shows an emission maximum at 662 nm, whereas in $CHCl_3$/MeOH mixture, the spectrum has the same shape but is red-shifted with a maximum at λ_{em} = 667 nm. In

DMSO, the emission band peaks at λ_{em} = 665 nm, is broader and lacks the shoulder around 730 nm. These spectra are independent of the excitation wavelenght.

9. Time Correlated Single Photon Counting (TCSPC)

Time-resolved fluorescence: Fluorescence decay measurements were performed using the same time-correlated single photon counting (TCSPC) setup as described in ref. S5. Excitation was carried out with o90 ps pulses generated with a laser diode at 395 nm (PicoQuant model LDH-PC-400B) and fluorescence was detected at magic angle. The full width at half-maximum (FWHM) of the instrument response function (IRF) was around 200 ps.

Fluorescence lifetime of NDI 1 in $CHCl_3$ and DMSO:

Figures S10 and S11 show the fluorescence decays of NDI **1** in $CHCl_3$ and in DMSO obtained using the Time Correlated Single Photon Counting (TCSPC) technique. Excitation was performed at 395 nm and the fluorescence was monitored at 650 nm.

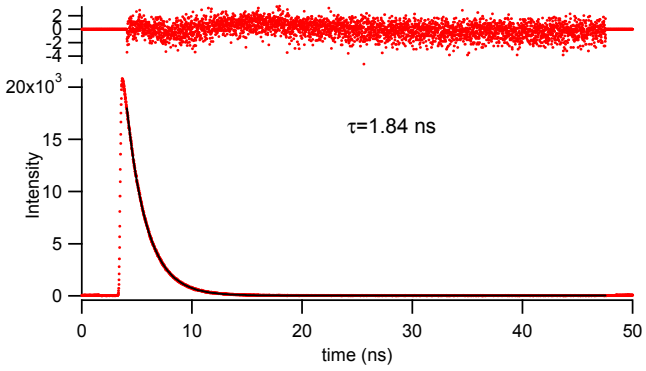

Figure S10. Fluorescence decay of NDI **1** in $CHCl_3$ observed at 650 nm after 395 nm excitation.

In $CHCl_3$, the decay can be well reproduced by a monoexponential function with a 1.84 ns lifetime.

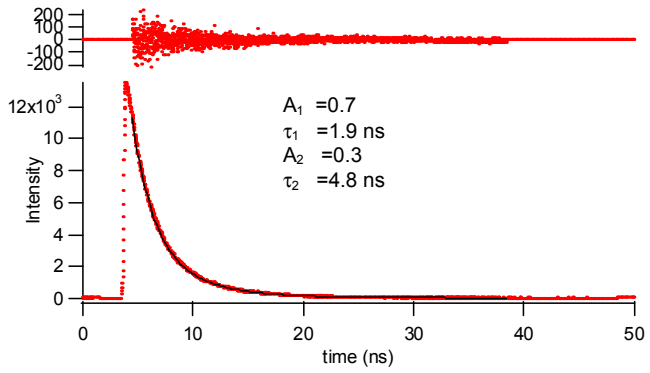

Figure S11. Fluorescence decay of SVB50 in DMSO observed at 650 nm after 395 nm excitation.

Two exponential functions were necessary to reproduce the fluorescence decay of NDI **1** in DMSO (figure S11) with the time constants lifetimes τ_1= 1.9 ns and τ_2= 4.8 ns and the relative amplitudes A_1=0.7 and A_2=0.3. This biexponential dynamics points to the existence of two emitting populations, one with a 1.9 ns lifetime like in $CHCl_3$ and one with a 4.8 ns lifetime. The latter might be due to the emission from the aggregated dyes.

10. Transient Absorption (TA)

Transient absorption (TA): The experimental setup has been described in detail earlier.[S6,S7] Excitation was performed at 400 nm with the frequencydoubled output of a standard 1 kHz amplified Ti: Sapphire system (Spectra-Physics) and at 615 nm with a home-built two-stage non-collinear optical parametric amplifier. The pump intensity on the sample was ca. 1–2 mJ cm^{-2}. The polarisation of the probe pulses was at magic angle

relative to that of the pump pulses. All spectra were corrected for the chirp of the white-light probe pulses. The FWHM of the response function was ca. 150 fs. The sample solutions were placed in a 1 mm thick quartz cell and were continuously stirred by N_2 bubbling. Their absorbance at the excitation wavelength was around 0.3.

TA spectra recorded at selected time delays after 630 nm excitation of NDI **1** in $CHCl_3$ are shown in figure S12.

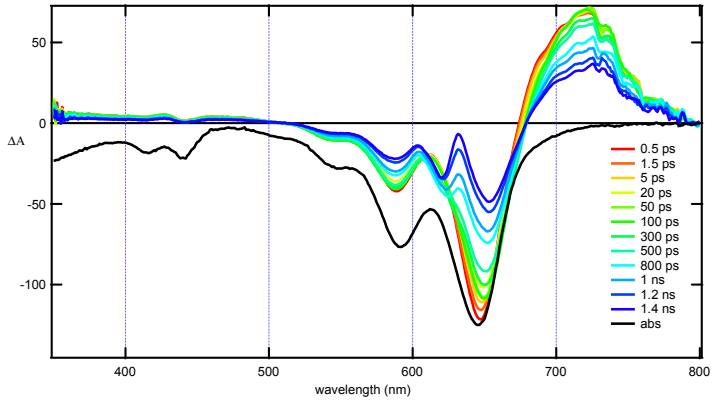

Figure S12. TA spectra measured with NDI **1** in $CHCl_3$ at various time delays after 630 nm excitation together with the inverted steady state absorption spectrum (black line). The feature around 630 nm is an artefact due to the scattered pump light.

The TA spectra show very weak positive features in the 350–500 region and a more intense one above 670 nm, that can all be assigned to excited-state absorption. The structured negative band between 520–700 nm is due to the bleach of the $S_1 \leftarrow S_0$ transition, whereas the bleach of the $S_2 \leftarrow S_0$ transition can be seen as indents at 411 and 440 nm. Apart from a small spectral dynamics on a short timescale, most probably associated with relaxation processes, the TA features decay exponentially to zero with a time constant >1 ns, in agreement with the fluorescence lifetime. The time window of the

TA experiment is too narrow to allow a precise determination of this ns time constant. Thus the TA spectrum shows essentially the decay of the excited-state population of NDI **1** back to the ground state. The TA spectra recorded in DMSO (figure S13) are very similar to those in $CHCl_3$ (figure S12). Here again, the TA dynamics is dominated by a component with a lifetime longer than >1 ns. The limited time window does not allow the slow decay component with 4.8 ns observed in the TCSPC measurement to be resolved.

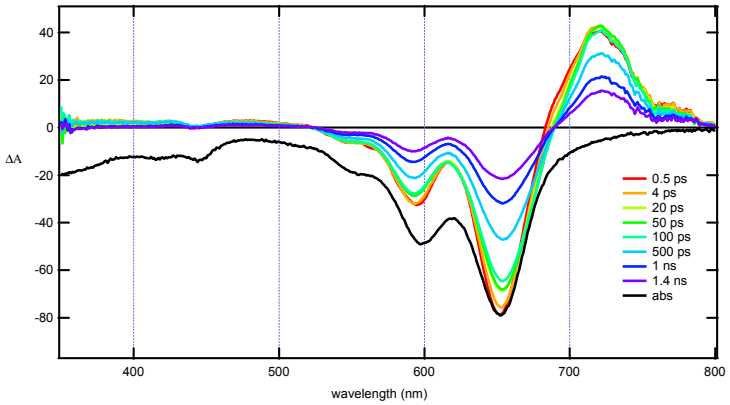

Figure 15. TA spectra of NDI **1** in DMSO at various time delays after 630 nm excitation together with the inverted steady state absorption spectrum (black line)

Typical NMR spectra of NDI 1

^{1}H NMR of NDI **1** in $CDCl_3$

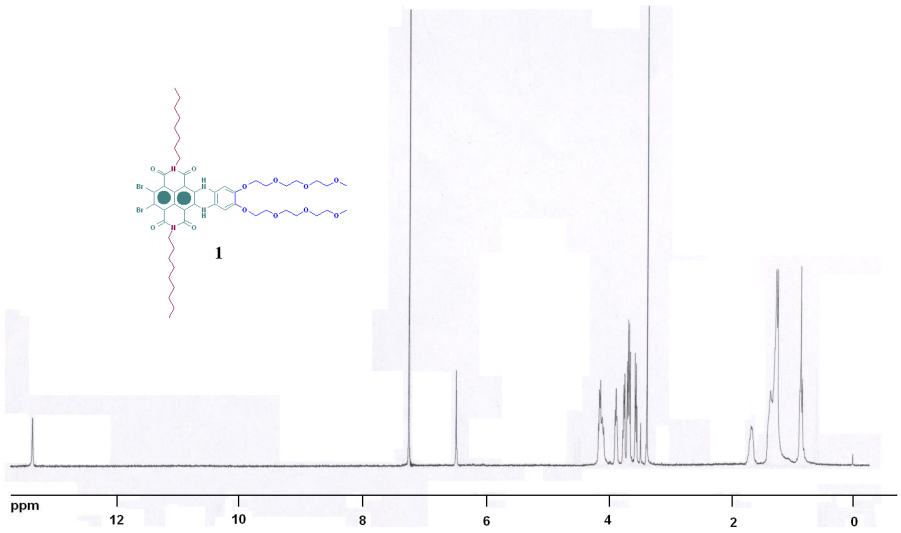

^{13}C NMR of NDI **1** in $CDCl_3$

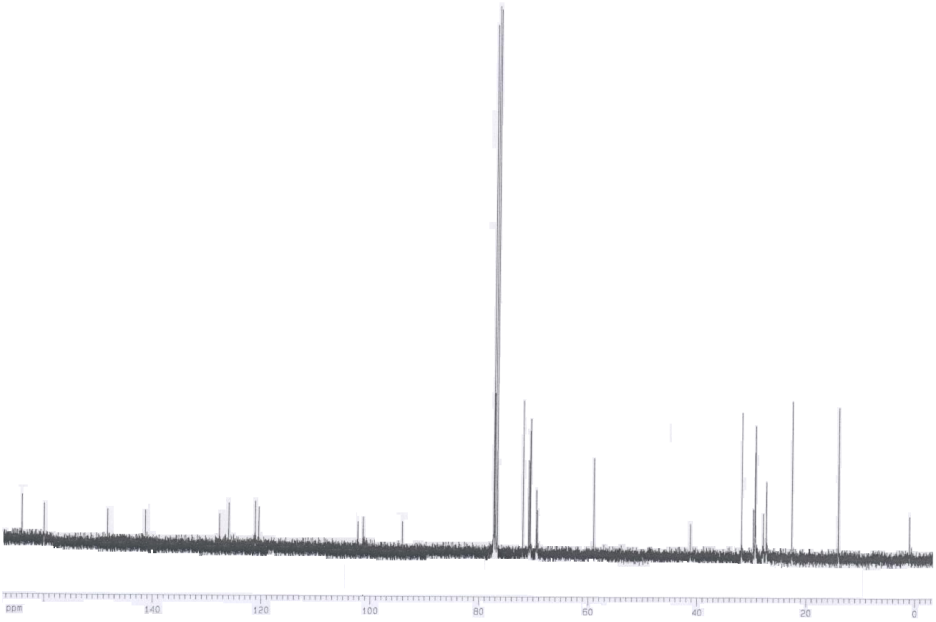

11. References

S1. (a) X. Gao, W. Qiu, X. Yang, Y. Liu, Y. Wang, H. Zhang, T. Qi, Y. Liu, K. Lu, C. Du, Z. Shuai, G. Yu, D. Zhu, *Org. Lett.*, 2007, **9**, 3917. (b) S. V. Bhosale, C. Jani, C. H. Lalander, S. J. Langford. *Chem. Commun.* 2010, **46**, 973.

S2. S. Ghosh, X.-Q. Li, V. Stepanenko, F. Würthner *Chem. Eur. J.* 2008, **14**, 11343.

S3. (a) L. Wang, H. Liu, J. Hao, *Chem. Commun.* 2009, 1353. (b) W. Cai, G.-T. Wang, Y.-X. Xu, X.-K. Jiang, Z.-T. Li, *J. Am. Chem. Soc.* 2008, **130**, 6936.

S4. (a) S. W. Provencher, *Biophys. J.* 1976, **16**, 27. (b) S. W. Provencher, *J. Chem. Phys.* 1976, **64**, 2772.

S5. I. Petkova, G. Dobrikov, N. Banerji, G. Duvanel, R. Perez, D. Dimitrov, P. Nikolov, E.Vauthey, *J. Phys. Chem. A*, 2010, **114**, 10-20.

S6. G. Duvanel, N. Banerji and E. Vauthey, J. Phys. Chem. A, 2007, **111**, 5361-5369.

S7. N. Banerji, G. Duvanel, A. Perez-Velasco, S. Maity, N. Sakai, S. Matile and E. Vauthey, J. Phys. Chem. A, 2009, **113**, 8202-8212